# Symmetry Breaking in Dense Solid Hydrogen: Mechanisms for the Transitions to Phase II and Phase III

Pierre Tolédano,[1] Hannelore Katzke,[2,*] Alexander F. Goncharov,[3] and Russell J. Hemley[3]

[1]*Physique des Systèmes Complexes, Université de Picardie, 33 rue Saint-Leu, 80000 Amiens, France*
[2]*Institute of Geosciences, Crystallography, University of Kiel, Olshausenstraße 40, 24098 Kiel, Germany*
[3]*Geophysical Laboratory, Carnegie Institution of Washington, Washington D.C. 20015, USA*

(Received 29 May 2009; revised manuscript received 16 July 2009; published 2 September 2009)

Spectroscopic data for the high-pressure phases of hydrogen together with the topology of the phase diagram provide new insight on the behavior of the material at megabar pressure. Structural mechanisms are proposed for the transitions to phases II and III. These mechanisms include a partially ordered structure (possibly incommensurate) and an ordered isotranslational structure for the two phases, respectively. The analysis supports the existence of an additional phase, isostructural to phase III, with boundary that meets to form a second triple point with phases I and III.

DOI: 10.1103/PhysRevLett.103.105301 PACS numbers: 67.80.F−, 62.50.−p, 64.70.kt

Despite important advances in our knowledge of solid hydrogen over the last decades [1–3], the structures of the high-pressure phases and features of the phase diagram are not yet understood. At megabar pressures hydrogen exhibits at least three different solid molecular phases. The lower pressure phase I consists of freely rotating molecules on a hexagonal close-packed (hcp) lattice [1,3]. Between about 110 and 150 GPa the broken-symmetry phase II with orientationally ordered molecules forms [4–6]. Above 150 GPa, phase III forms [7,8]; it has a distinct vibrational spectrum [5] and remains stable up to at least 320 GPa [9,10]. Numerous first-principles calculations have been performed to describe the structures of phases II and III [11–19]. Here we show that symmetry considerations provide important constraints on structural models for the different solid phases. A Landau-type analysis of related transition mechanisms yields a theoretical phase diagram that provides new insight into the high-pressure behavior of hydrogen.

Experimental observations and symmetry considerations drastically reduce the number of possible structural symmetries of phases II and III. The character of the changes in vibrational spectra [7,20] and the reported evidence for small discontinuities in $d$ spacings at the I → II and II → III transitions [6,21] provide additional constraints. Specifically, the spectroscopic and diffraction data exclude major reconstructive mechanisms, suggesting that group-subgroup relationships are preserved between the three phases, as is the case for many order-disorder transitions [22]. The distributions of Raman and infrared active modes [5,9,23,24] indicate that the orientational order in phases II and III are qualitatively different, with increasing order in phase III [5,23]. The transitions leading to these phases can thus be assumed to involve distinct symmetry-breaking order parameters. We explore the consequences of assuming that unifying ordering mechanisms from the disordered structure of phase I lead to the structures of phases II and III in which the hcp structure of the molecular centers remains almost unaffected [5,24]. The vibrational properties of phase II imply the presence of an inversion center, and a multiplication by at least a factor of 2 of the number of molecules in the primitive cell relative to phase I [5]. The spectral changes observed in phase III indicate that its primitive cell contains at least four molecules [5]. A group-theoretical analysis of the structural mechanisms induced by the irreducible representations of the $P6_3/mmc$ space group of phase I yields structures that fulfill the above conditions.

To begin, we view the hcp structure of phase I as a spherical distribution of $H_2$ molecules containing seven, energetically equivalent orientations at the experimentally determined bond lengths [Fig. 1(a)] [1]. An ordering transition to phase II yields a partially ordered structure [Fig. 1(b)] with symmetry $Cmcm$ and eight molecules in the primitive unit cell, the orthorhombic deformation $e_{xx}$-$e_{yy}$ coinciding with the displacement of the $E_{2g}$ optical phonon. The increased number of molecules per unit cell relative to phase I is consistent with the low-frequency librons and with the second Raman [5] and the sharp IR vibrons observed in phase II [2]. Weak spectral changes and the specific ordering in phase II could be affected by ortho-para state or residual strain. The intensity decrease in the Raman phonon and the main IR vibron in phase II [5] is also naturally explained by specific selection rules arising from the presence of molecules with different site symmetries in $Cmcm$ structures. At the I → II transition, the molecules adopt one among the seven possible orientations existing in phase I, and may order over two energetically equivalent orientations in the basal plane of a trigonal bipyramid, the molecular centers forming a slightly deformed hcp lattice. This may induce a topological frustration giving rise to the long-period incommensurability along **a**, consistent with superlattice reflections observed by neutron and x-ray measurements in phase II of $D_2$ [6]. An incommensurate phase II would display the superspace group symmetry $Cmcm(\alpha 00)$.

 

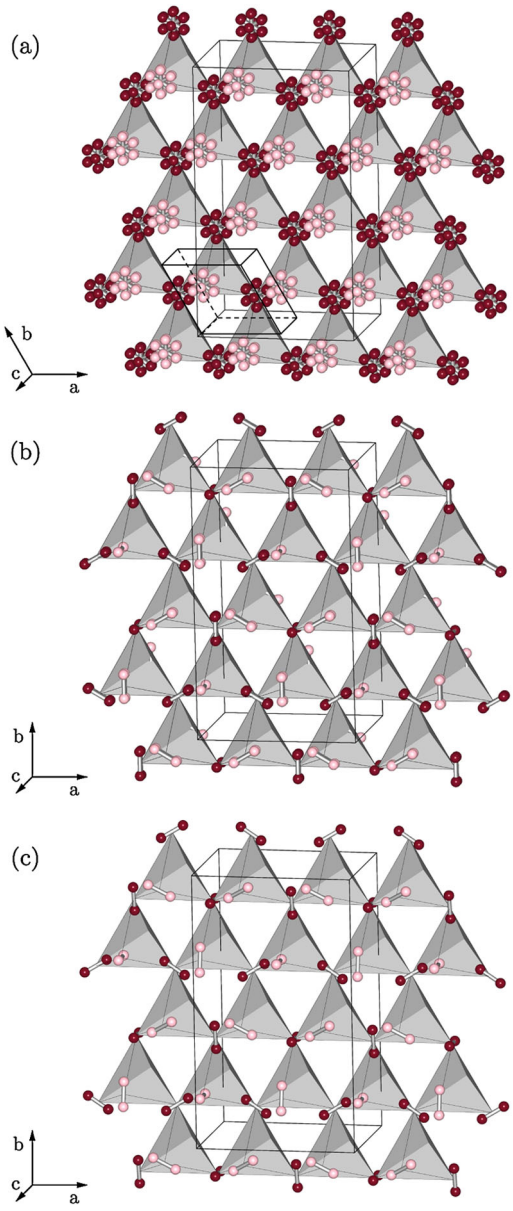


FIG. 1 (color online). Symmetry considerations for structures considered for phases I, II, and III of dense solid $H_2$. (a) The disordered structure of I. The hexagonal unit cell, shown by thick lines, contains two molecules centered at the Wyckoff position $2d$. The H atoms partly occupy one Wyckoff position $4f$ and two positions $12k$ of space group $P6_3/mmc$. (b) A structural model for the partially ordered broken-symmetry phase. In this model the conventional orthorhombic unit cell contains 16 molecules and the 32 H-atoms are distributed over one fully occupied $8f$, two half-filled $8f$ and two half-filled $16h$ positions. (c) The $Cmc2_1$ structure with 16 molecules in the conventional unit cell; in its fully ordered structure the H atoms would occupy four Wyckoff positions $4a$ and two positions $8b$.

Extending the above analysis to phase III leads to a structure with space group $Cmc2_1$ with eight molecules per unit cell [Fig. 1(c)]. The seven different orientations with the molecular axes pointing to the midpoints of the upper and lower tetrahedron of a trigonal bipyramid are all

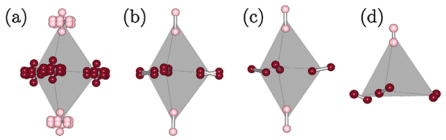


FIG. 2 (color online). Orientational order for displacive transition models for phases I, II, and III and the cubic $Pa\bar{3}$ structure. (a) Spherical electron density of phase I modeled by disordering the molecules over seven energetically equivalent orientations with the molecular axes directing towards the centers of the upper and lower tetrahedrons of a trigonal bipyramid. (b) For phase II, the molecules in the basal planes of the bipyramids adopt one of two possible energetically equivalent orientations that may result in a topological frustration giving rise to an incommensurate structure. (c) Orientational order of phase III, in which the molecules are fully ordered. (d) $Pa\bar{3}$-ordering in $H_2$. The four orientations correspond to the symmetry-equivalent high-symmetry $\langle 111 \rangle$ directions in the cubic lattice.

realized in an ordered manner, the $H_2$ molecules locking to one of the two orientations available in phase II. The strong IR vibron absorption observed in phase III relative to phase II [5] then arises from the different crystallographic environment of the atoms at the molecular ends in the corresponding structures (e.g., Refs [2,23]). In both structures the molecular ends differ; however, due to the quantum disorder in phase II the symmetry-equivalent atoms have all the same environment, whereas the atoms in phase III have different surroundings in the second coordination sphere [23]. Group-theoretical analysis for phase III predicts sufficient phonon, librational, and vibron modes to match the observed Raman and IR spectra [2,5]. Figure 2 summarizes the orientational order of the $H_2$ molecules that follows from this approach. The molecular order in the orthorhombically deformed hexagonal layers of phases II and III matches that of the hexagonal layers of the $Pa\bar{3}$ structure of o-$H_2$ [Fig. 2(d)] found below 3.8 K at ambient pressure and in $\alpha$-$N_2$ [25].

The proposed structures of phases II and III are described by two distinct irreducible representations of the $P6_3/mmc$ space group at the $M$ point $(4\pi/3a, 2\pi/3a, 0)$ of the hexagonal Brillouin-zone surface, labeled $M_1^+$ and $M_2^-$, corresponding to three-component order parameters, denoted $(\eta_1, \eta_2, \eta_3)$ and $(\zeta_1, \zeta_2, \zeta_3)$. The $Cmcm$ structure for phase II is stabilized for $\eta_1 = \eta_2 \neq \eta_3$ [26]. It has the basic translations $(2a, 2a + 4b, c)$ for the conventional $C$ cell. The $Cmc2_1$ structure is isotranslational to that of the lower pressure phase and corresponds to $\zeta_1 = \zeta_2 \neq \zeta_3$. Accordingly, the *effective* Landau free-energy associated with the transitions between these structures reads

$$\begin{aligned} F_1(T, P, \eta_i, \zeta_i) = {} & F_0(T, P) + a_1(2\eta_1^2 + \eta_3^2) + a_2\eta_1^2\eta_3 \\ & + a_3(2\eta_1^2 + \eta_3^2)^2 + a_4(2\eta_1^4 + \eta_3^4) \\ & + b_1(2\zeta_1^2 + \zeta_3^2) + b_2(2\zeta_1^2 + \zeta_3^2)^2 \\ & + b_3(2\zeta_1^4 + \zeta_3^4) + b_4\zeta_1^4\zeta_3^2 \\ & + c(2\eta_1\zeta_1^2 + \eta_3\zeta_3^2). \end{aligned} \quad (1)$$

First-order transitions between the phases require truncating $F_1$ at the sixth and fourth degrees in the $\zeta_i$ and $\eta_i$ components, respectively. The $c$-coupling is necessary for describing the $Cmcm \rightarrow Cmc2_1$ transition. Minimizing $F_1$ with respect to $\eta_i$ and $\zeta_i$ shows that the $Cmcm$ structure is stable for $\eta_i \neq 0$, $\zeta_i = 0$, whereas $Cmc2_1$ is stable for $\eta_i \neq 0$ *and* $\zeta_i \neq 0$. A consequence of this assignment of structure for $H_2$ is that full ordering of the molecules in the latter cannot take place independently of the partial ordering mechanism in the former. Two different paths can be distinguished: At the II $\rightarrow$ III transition a rapid increase of the full ordering process should be observed, since the partial ordering represented by $\eta_i$ is almost achieved. By contrast, at the transition from $P63/mmc$ to $Cmc2_1$ the symmetry-breaking mechanisms associated with the $\eta_i$ and $\zeta_i$ order parameters take place simultaneously and the full ordering process should occur progressively. The topology of the phase diagram associated with $F_1$ remains unchanged when assuming $\eta_1 = \eta_3 = \eta$ and $\zeta_1 = \zeta_3 = \zeta$. $F_1$ then reduces to

$$F_2(T, P, \eta, \zeta) = F_0(T, P) + \frac{\alpha_1}{2}\eta^2 + \frac{\beta_1}{3}\eta^3 + \frac{\gamma_1}{4}\eta^4 + \frac{\alpha_2}{2}\zeta^2 + \frac{\beta_2}{4}\zeta^4 + \frac{\gamma_2}{6}\zeta^6 + \delta\eta\zeta^2. \quad (2)$$

Figure 3 shows the theoretical phase diagram deduced from the minimization of $F_2$ with respect to $\eta$ and $\zeta$, under definite stability conditions for the coefficients $\alpha_i$, $\beta_i$, $\gamma_i$, and $\delta$. It differs from the experimental phase diagram of hydrogen by the proposed existence of additional invariant points along the I-III phase line [20]. Specifically, there is evidence for an additional phase I′, separated from phase I by a first-order transition line that merges with phases I and III at a second triple point ($T_2$). Phase I′ was suggested in $D_2$ based on measured changes in slope of the I-III line and a 10 $cm^{-1}$ vibron discontinuity [20]; the proposal was subsequently supported by first-principles simulations [16]. More recently, evidence for I′ was reported by coherent anti-Stokes Raman spectroscopy [27] (see also Ref. [28]). The different symmetries of phases I and III exclude passing continuously from phase I to III beyond a proposed second invariant point, the critical end point $C$. If we assume that phases I′ and III are isosymmetric, their structures correspond to different equilibrium values of the order parameters ($\eta$, $\zeta$) and ($\eta'$, $\zeta'$), reflecting different stages in the ordering process. Far from the critical point, the proposed phase I′ is less ordered than phase III. At the critical point ($\eta = \eta'$, $\zeta = \zeta'$) the molecular order is fully realized for the two phases.

Insight into the experimental phase diagram of hydrogen can be obtained from the theoretical diagram by a *linear* transformation that preserves its topological singularities. If we assume a linear dependence on temperature and pressure of the coefficients $\alpha_1(T, P)$ and $\alpha_2(T, P)$, which is valid close to the singularities, we can see why in the theoretical phase diagram the I $\rightarrow$ II first-order transition

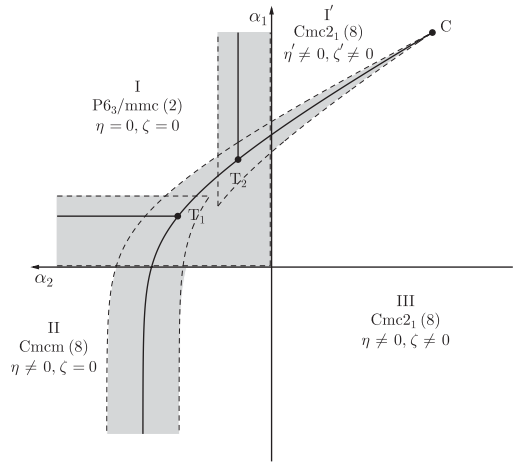


FIG. 3. Theoretical phase diagram in the ($\alpha_1$, $\alpha_2$) plane deduced from the minimization with respect to $\eta$ and $\zeta$, of the free-energy $F_2(T, P, \eta, \zeta)$ given by Eq. (2), for $\beta_1 > 0$, $\beta_2 < 0$, $\gamma_1 > 0$, $\gamma_2 = 1$ and $\delta > 0$. Solid and hatched curves represent, respectively, first-order transition and limit of stability lines. Phase coexistence regions are in gray. The space group (number of molecules in the primitive cell) and equilibrium values of the order parameters $\eta$ and $\zeta$ are indicated for each phase. Phase I is stable for $\alpha_1 > 0$ and $\alpha_2 > 0$ and transforms into phase II across the first-order transition line $\alpha_1 = 2\beta_1^2/9\gamma_1$, which merges with phase III at the triple point $T_1$. The equilibrium values of the order parameter ($\eta$, $\zeta$) in phases III and I′ are solutions of the coupled equations: $\eta(\alpha_1 + \beta_1\eta + \gamma_1\eta^2) + \delta\zeta^2 = 0$ and $\alpha_2 + \beta_2\zeta^2 + \gamma_2\zeta^4 + 2\delta\eta = 0$. The I′ $\rightarrow$ III isostructural transition line ends at the critical point $C$, merging with phase I at the triple point $T_2$. The first-order transition curve II $\rightarrow$ III corresponds to a parabolic branch whereas the possible I $\rightarrow$ I′ transition line merges at $T_2$ with phase III.

curve corresponds to the straight line $\alpha_1 = \frac{2\beta_1^2}{9\gamma_1}$, whereas experimentally for hydrogen the transition curve separating phases I and II decreases with temperature and pressure far from the triple point $T_1$. Close to the triple point the I $\rightarrow$ II transition line varies linearly in $P$-$T$, 140–162 GPa for $D_2$ [20]. The topology of theoretical phase diagram of Fig. 3 thus reflects key features of the phase diagram of hydrogen, i.e., the existence of a critical point ending a first-order isostructural transition line, for example, at $P_c = 192$ GPa and $T_c = 265$ K in $D_2$ [20]. However, our phenomenological Landau approach, which expresses the macroscopic properties of the system, cannot account for the mass dependence of the I $\rightarrow$ II transition and mass independence of the II $\rightarrow$ III transition, which relate to the quantum properties of hydrogen and require a microscopic model, as proposed, for example, by Edwards and Ashcroft [17]. By contrast, these properties are reflected in the remaining positional disorder assumed in the structure of phase II, which disappears in phase III.

A number of different structures of phases II and III have been proposed on the basis of first-principles calculations that display no direct group-subgroup relationship with the

structure of phase I. This is the case for the $Pca2_1$ ($Z = 8$) structure proposed for phase II [11–13], and for the related $Pca2_1$ ($Z = 16$) structure considered for phase III [14]. Both structures can be derived from the $Pa\bar{3}$ ($Z = 8$) structure of $H_2$, which has been also considered in structural models of phase II [5,15]. The structure of phase II may also depend on residual $J = 1$ molecule concentration. Other structural symmetries have been considered theoretically for phase II ($A2/a$ ($Z = 64$) [16], $P2_1/c$ ($Z = 8$) [17]) and phase III ($Cmc2_1$ ($Z = 8$) [18], $Cmca$ ($Z = 12$) [19], $C2/c$ ($Z = 24$) [19]).

None of these structures is induced by an irreducible representation of the $P6_3/mmc$ space group, which implies that they result from an indirect reconstructive mechanism. Our proposed $Cmcm$ and $Cmc2_1$ symmetries correspond to the limited set of structures verifying the full set of available experimental and topological constraints for continuous I → II and II → III transitions, although one cannot exclude further lowering of the symmetries associated with possible secondary displacements. Experimental signatures of these structures are the fourfold primitive isotranslational unit cells assumed for phases II and III, the typical dielectric anomalies that should be observed at the II → III *proper* ferroelectric transition, or the existence of three and six ferroelastic domains that should arise, respectively, at the I → II and I → III transitions.

In summary, currently available experimental observations combined with topological considerations and a Landau-theoretical analysis yield new constraints on the structures of phases II and III. Landau treatments of the transition have been considered previously but predate the availability of spectroscopic data needed to constrain the structures [29]. A partially ordered and possibly incommensurate, structure with space group $Cmcm$, and a fully ordered isotranslational ferroelectric structure with lower $Cmc2_1$ symmetry follow naturally if the transitions occur between symmetry related structures. An additional phase line associated with I′ could merge to form a second triple point with phases I and III. This intermediate phase is required if the I-III line terminates at a true critical point. Therefore, our theoretical work represents a significant advance in relating organically detailed structures of phases II and III to the actual phase diagram. It provides a number of precise structural and topological indications that should stimulate further experimental verifications.

This work was supported by the German Science Foundation under DE 412/33-1, NSF-DMR, DOE-NNSA (CDAC), and the Carnegie Institution.

*hanne@min.uni-kiel.de

[1] J. Van Kranendonk, *Solid Hydrogen* (Plenum, New York, 1983).
[2] H. K. Mao and R. J. Hemley, Rev. Mod. Phys. **66**, 671 (1994).
[3] A. F. Goncharov and J. C. Crowhurst, Phase Transit. **80**, 1051 (2007); R. J. Hemley, Proceedings of the 2008 Scottish Universities Summer School in Physics (to be published).
[4] H. E. Lorenzana, I. F.Silvera, and K. A. Goettel, Phys. Rev. Lett. **64**, 1939 (1990).
[5] A. F. Goncharov, R. J. Hemley, H. K. Mao, and J. F. Shu, Phys. Rev. Lett. **80**, 101 (1998).
[6] I. Goncharenko and P. Loubeyre, Nature (London) **435**, 1206 (2005).
[7] R. J. Hemley and H. K. Mao, Phys. Rev. Lett. **61**, 857 (1988); H. E. Lorenzana, I. F. Silvera, and K. A. Goettel, Phys. Rev. Lett. **63**, 2080 (1989).
[8] M. Hanfland, R. J. Hemley, and H. K. Mao, Phys. Rev. Lett. **70**, 3760 (1993); R. J. Hemley, Z. G. Soos, M. Hanfland, and H. K. Mao, Nature (London) **369**, 384 (1994); N. H. Chen, E. Sterer, and I. F. Silvera, Phys. Rev. Lett. **76**, 1663 (1996).
[9] A. F. Goncharov, E. Gregoryanz, R. J. Hemley, and H. K. Mao, Proc. Natl. Acad. Sci. U.S.A. **98**, 14 234 (2001).
[10] P. Loubeyre, F. Occelli, and R. LeToullec, Nature (London) **416**, 613 (2002).
[11] J. Kohanoff, S. Scandolo, G. L. Chiarotti, and E. Tosatti, Phys. Rev. Lett. **78**, 2783 (1997).
[12] K. Nagao, T. Takezawa, and H. Nagara, Phys. Rev. B **59**, 13741 (1999).
[13] M. Stadele and R. M. Martin, Phys. Rev. Lett. **84**, 6070 (2000).
[14] J. Kohanoff, S. Scandolo, S. de Gironcoli, and E. Tosatti, Phys. Rev. Lett. **83**, 4097 (1999).
[15] T. Cui, E. Cheng, B. J.Alder, and K. B. Whaley, Phys. Rev. B **55**, 12 253 (1997).
[16] M. P. Surh, K. J. Runge, T. W. Barbee, E. L. Pollock, and C. Mailhiot, Phys. Rev. B **55**, 11 330 (1997).
[17] B. Edwards and N. W. Ashcroft, Proc. Natl. Acad. Sci. U.S.A. **101**, 4013 (2004).
[18] H. Kitamura, S. Tsuneyuki, O. Tadashi, and T. Miyake, Nature (London) **404**, 259 (2000).
[19] C. J. Pickard and R. J. Needs, Nature Phys. **3**, 473 (2007).
[20] A. F. Goncharov, I. I. Mazin, J. H. Eggert, R. J. Hemley, and H. K. Mao, Phys. Rev. Lett. **75**, 2514 (1995).
[21] P. Loubeyre, F. Occelli, and M. Mezouar (unpublished).
[22] N. G. Parsonage and L. A. K. Staveley, *Disorder in Crystals* (Oxford University Press, Oxford, 1976).
[23] I. I. Mazin, R. J. Hemley, A. F. Goncharov, M. Hanfland, and H. K. Mao, Phys. Rev. Lett. **78**, 1066 (1997); R. J. Hemley *et al.*, Europhys. Lett. **37**, 403 (1997).
[24] A. F. Goncharov, M. A. Strzhemechny, H. K. Mao, and R. J. Hemley, Phys. Rev. B **63**, 064304 (2001).
[25] H. Katzke and P. Tolédano, Phys. Rev. B **78**, 064103 (2008).
[26] H. T. Stokes and D. M. Hatch, *Isotropy Subgroups of the 230 Crystallographic Space Groups* (World Scientific, Singapore, 1988).
[27] B. J. Baer, W. J. Evans, and C. S. Yoo, Phys. Rev. Lett. **98**, 235503 (2007).
[28] A. F. Goncharov, R. J. Hemley, and H. K. Mao (to be published).
[29] H. E. Lorenzana and R. Jeanloz, J. Chem. Phys. **95**, 3838 (1991).